

Expression of ezrin correlates with malignant phenotype of lung cancer, and in vitro knockdown of ezrin reverses the aggressive biological behavior of lung cancer cells

Qingchang Li · Hui Gao · Hongtao Xu · Xin Wang ·
Yongqi Pan · Fengxia Hao · Xueshan Qiu ·
Maggie Stoecker · Endi Wang · Enhua Wang

Received: 13 February 2012 / Accepted: 3 April 2012 / Published online: 20 April 2012
© International Society of Oncology and BioMarkers (ISOBM) 2012

Abstract Ezrin, one of the ezrin–radixin–moesin proteins, is involved in the formation of cell membrane processes such as lamellipodia and filopodia and acts as a membrane–cytoskeleton linker. Its aberrant expression correlates with development and progression of several human cancers. However, the expression of ezrin and its role in lung cancer are currently unknown. In this study, we performed ezrin small interfering RNA transfection in two lung cancer cell lines and examined the effects on malignant phenotypes in cancer cells by using 3-(4,5-dimethylthiazol-2-yl)-2,5-diphenyltetrazolium bromide, wound healing, and chamber transwell assays. Ezrin knockdown significantly reduced the proliferation, migration, and invasion of lung cancer cells in vitro. To address the possible mechanisms, we evaluated the expression of adhesion molecules E-cadherin and β -catenin by Western blot and reverse transcriptase-polymerase chain reaction analyses. The results demonstrated that downregulation of ezrin reduced β -catenin and increased E-cadherin at the protein level but had no effects on their mRNA levels, suggesting posttranscriptional regulation of these two

adhesion molecules. Immunofluorescence assays revealed that ezrin knockdown restored membranous expression of E-cadherin and decreased cytoplasmic β -catenin in lung cancer cells. In addition, ezrin expression was immunohistochemically evaluated on 135 normal and 183 lung cancer tissues. The expression of ezrin was significantly higher in cancer samples than paired autologous normal lung tissues. In normal bronchial epithelium, ezrin was mainly localized on the apical membrane, while in lung cancers and metastatic foci, ezrin was primarily distributed in cytoplasm. Among lung cancer tissues, expression of ezrin was higher in the invasive front of primary lesions and the highest in lymphatic metastasis. Statistical analysis demonstrated that ezrin expression correlated significantly with lymphatic metastasis and advanced TNM stage. Our data suggest that ezrin may play a crucial role in governing the biological behavior of lung cancer.

Keywords Ezrin · Lung cancer · Metastasis · Cell adhesion · Tumor progression

Q. Li · H. Gao · H. Xu · X. Wang · Y. Pan · F. Hao · X. Qiu ·
E. Wang (✉)
Department of Pathology, The First Affiliated Hospital
and College of Basic Medical Sciences, China Medical University,
Shenyang 110001, China
e-mail: wangeh@hotmail.com

Q. Li · H. Gao · H. Xu · X. Wang · Y. Pan · F. Hao · X. Qiu ·
E. Wang
Institute of Pathology and Pathophysiology,
China Medical University,
Shenyang 110001, China

M. Stoecker · E. Wang
Department of Pathology, Duke University Medical Center,
Durham, NC 27710, USA

Abbreviations

BSA	Bovine serum albumin
ERM	Ezrin–radixin–moesin
ICAM	Intercellular adhesion molecule
siRNA	Small interfering RNA
DMSO	Dimethyl sulfoxide
DAB	Diaminobenzidine
PVDF	Polyvinylidene fluoride
HRP	Horseradish peroxidase
EB	Ethidium bromide
NSCLC	Non-small cell lung cancer
FCS	Fetal calf serum
FITC	Fluorescein isothiocyanate

Introduction

Lung cancer is a leading cause of cancer-related mortality worldwide. In patients with lung cancer, tumor metastasis is associated with a poor prognosis [1]. Despite significant advances in early diagnosis and treatment of primary human lung cancer, prevention of metastasis and eradication of micrometastases remains a challenge in clinical management. During the process of metastasis, cancer cells invade surrounding normal tissue, recruit new blood vessels, and migrate to and eventually colonize the distant organs/tissues [2]. Each of these steps involves a substantial interaction between neoplastic cells and adjacent non-neoplastic tissues. Currently, increased evidence suggests that membrane–cytoskeleton linker ezrin plays a pivotal role in tumor invasion and metastasis [3].

Ezrin, which is encoded by the *vil2* (EZR) gene, is a member of the ezrin–radixin–moesin (ERM) protein family and was initially thought to be a simple cross-linker between actin filaments and other membrane proteins. Recent studies have demonstrated that ezrin may be involved in cell signal transduction, development, and differentiation [4]. For instance, laboratory investigations have revealed that upregulation of ezrin is associated with proliferation and immortalization of fibroblasts [5] and correlates with the acquisition of an invasive phenotype in transformed esophageal epithelial cells [6] and endometrial cancer cells [7]. In addition, overexpression of ezrin has been shown to enhance metastatic potential in various types of malignant tumors, including osteosarcoma [8], rhabdomyosarcoma [9, 10], and carcinomas of the pancreas [11], ovary [12], and endometrium [13].

Several studies have implicated ERM proteins in the regulation of cell–cell and cell–matrix adhesion. Overexpression of ezrin has been shown to disrupt cell–cell adhesion, and its suppression facilitates adhesion [14]. Ezrin is known to function as an organizer of cell–cell adherent junctions and may play a key role in metastasis of epithelial neoplasms. Loss of E-cadherin or deregulation of its function by blocking its downstream signaling is thought to promote tumor metastasis. It has been reported that silencing of ezrin induces increased expression of E-cadherin and decreased phosphorylation of β -catenin by inhibiting phosphorylation of c-src [15]. It has also been shown that ezrin protein controls cell adhesion via different mechanisms. For instance, ezrin could modulate cell adhesion by interacting with intercellular adhesion molecule ICAM-2 [16] or by interacting with CD43 at cell adherens junctions [17, 18]. In addition, ezrin protein has been shown to regulate cell adhesion through Rho GTPase pathway [19].

In order to assess the role of ezrin in lung cancer, we used small interfering RNAs (siRNAs) against ezrin to study the impact of transient ezrin knockdown on proliferation and

invasion of lung cancer cells. We used immunofluorescence and Western blot methods to investigate the role of ezrin in expression and localization of E-cadherin and β -catenin proteins. We also performed immunohistochemical analysis in 135 tissue microarray specimens and 48 diagnostic tissue sections to investigate the relationship between ezrin expression and clinicopathological factors.

Materials and methods

Cells and culture conditions

Human lung adenocarcinoma cell lines LTEP- α -1 (LTE) and A549, human large cell lung cancer cell line NCI-H460 (H460), and human small cell lung cancer cell line NCI-H446 were obtained from American Type Culture Collection (Manassas, VA, USA). Human adenocarcinoma cell line SPC and large cell lung cancer line BE1 were purchased from the Cell Bank of Chinese Academy of Science (Shanghai, China). Cells were cultured in RPMI 1640 medium (Invitrogen, Carlsbad, CA) supplemented with 10 % fetal calf serum (Invitrogen), 100 IU/ml penicillin (Sigma, St. Louis, MO), and 100 μ g/ml streptomycin (Sigma). All cells were incubated at 37°C in a humidified atmosphere containing 5 % CO₂. For all experiments, the cells were growing in exponential phase.

Tissue specimen and immunohistochemical analysis

Tissue microarrays containing 135 lung cancer tissues and their adjacent normal lung tissues were purchased from Shanghai Outdo Biotech Co., Ltd (lot number: OD-CT-DgLug01-007 and OD-CT-DgLug01-008). Forty-eight surgically resected lung cancer specimens and their metastatic lymph nodes were obtained from Liaoning Provincial People's Hospital. All 183 formalin-fixed and paraffin-embedded human lung cancer specimens were analyzed by immunohistochemical staining for ezrin.

The sections were deparaffinized with xylene, rehydrated with graded alcohols, and rinsed with distilled water. Endogenous peroxidase was blocked with 3 % H₂O₂ in phosphate-buffered saline (PBS) for 15 min, followed by PBS wash three times. Antigen retrieval was done with high citrate buffer (DAKO Cytomation) for 30 min using a decloaking chamber (Biocare Medical). Sections were blocked with 10 % normal serum diluted with 2 % bovine serum albumin–PBS for 30 min at room temperature. The rabbit monoclonal ezrin antibody was applied (1:200) onto the sections overnight at 4°C. A biotinylated goat anti-rabbit immunoglobulin gamma (IgG) was used as secondary antibody and incubated for 30 min, followed by rinsing and incubating with avidin–biotin–peroxidase complex for

another 30 min. The sections were then developed with the liquid DAB substrate chromogen system (Maxim Bio, Inc.). The nucleus was counterstained with hematoxylin for 6 min. The negative controls were incubated with non-immune mouse IgG in place of the primary antibody. The immunostained slides were examined under the light microscope and scored independently by two experienced pathologists.

Judging criteria of immunohistochemical results, five \times 200 fields were randomly selected on each slide under the light microscope and 100 cells were counted in each field. The staining intensities were divided into colorless for 0 point, light yellow or yellow for 1 point, and brown for 2 points. Less than 10 % positivity in the cells is scored as 0, 10–50 % as 1, and more than 50 % as 2. After multiplying the two scores, if the product was more than 2, the case was graded as positive (+), and if it was less than 2, the case was graded as negative (–).

Western blot analysis

Cells were grown in 60-mm tissue culture plates, harvested after 48 h of incubation and lysed in CellLytic M Cell Lysis Reagent (Sigma-Aldrich). Fifty micrograms of protein extract was loaded onto each lane of a 10 % SDS-PAGE gel and separated by electrophoresis. The separated protein was then transferred to a PVDF membrane (Millipore, Bedford, MA) at 1.9 mA/cm² for 1.5 h with a semidry transfer cell (ATTO, Tokyo, Japan). After blocking with 5 % nonfat skim milk in TBS-T buffer overnight, the membrane was incubated with a primary antibody for 2 h, then with HRP-conjugated anti-rabbit or anti-mouse IgG antibody (GE Healthcare Bio-Sciences) at a dilution of 1:2,000 for 1 h. The membrane was extensively washed with TBS-T buffer, and the protein–antibody complex was visualized with an ECL detection reagent (GE Healthcare Bio-Sciences).

The following primary antibodies were used: rabbit monoclonal ezrin antibody (1:800, catalog number 1940-1, Epitomics biotech company, USA), mouse monoclonal β -catenin antibody (1:1000, catalog number sc-59896, Santa Cruz, CA), and mouse monoclonal E-cadherin antibody (1:200, catalog number sc-8426, Santa Cruz, CA). The secondary antibodies included rhodamine-conjugated goat anti-mouse and anti-rabbit (1:2,000, each, ZhongShan Biotechnology, Beijing).

Cell transfection with ezrin siRNA

Cells (2×10^5) were seeded in 2 ml antibiotic-free normal growth medium with 10 % FBS on a six-well tissue culture plate 24 h before transfection. For cell transfection, 6 μ l ezrin siRNA duplex (60 pmols siRNA) (sc-35349, Santa

Cruz Biotechnology Inc, CA) or control non-specific siRNA (sc-37007) together with 6 μ l siRNA transfection reagent (sc-29528) was added into 100 μ l siRNA transfection medium (sc-36868). After incubation of the mixture for 20 min at room temperature, the transfection mixture was added into the wells containing seeded cells and incubated together for 6 h at 37°C in a CO₂ incubator. One milliliter of normal growth medium containing two times the normal serum and antibiotics concentration (two times normal growth medium) was then added to the cultured wells without removing the transfection mixture.

Wound healing assay

Cells were plated onto 12-well tissue culture plates at 95 % confluence in complete tissue culture medium. After the cells became confluent, cell wounds were created by scratching cells using a micropipette tip. The medium was then immediately replaced, and spontaneous cell migration was monitored using a Nikon inverted microscope at 0, 6, and 24 h. The distance of wound closure was measured in three independent wound sites per group. Relative cell motility was calculated as the wound width at time (t) = 0 h minus the wound width at time (t) = 24 h.

In vitro invasion assays

Invasion assays were performed with 8.0 μ m pore inserts in 24-well BioCoat Chambers (Becton Dickinson) coated with 30 μ l of matrigel. Cells (1×10^4) in serum-free DMEM were placed in the upper transwell chambers, and the DMEM medium with 10 % FCS was placed in the lower chambers as a chemoattractant. The cells were removed from the upper surface of the filter by scraping with a cotton swab after 16 h. Migrated cells and invasive cells were fixed and stained with the crystal violet reagent. Cells that appeared on the lower surface of the filter were counted in ten random high power fields (magnification, $\times 400$) using an inverted microscope (Olympus IX51, Tokyo, Japan).

Cell growth assay

3-(4,5-Dimethylthiazol-2-yl)-2,5-diphenyltetrazolium bromide (MTT) assay was used for measuring cell proliferation. Cells grown on 96-well plate at a density of 3×10^3 cells per well were cultured and monitored daily for 4 days after plating. The absorbance, which correlates directly to the number of living cells in the culture, was measured at 550 nm using a microplate reader (Model 550, Bio-Rad, Hercules, CA, USA). A blank with dimethyl sulfoxide (DMSO) alone served as a control and its absorbance reading was subtracted from all values.

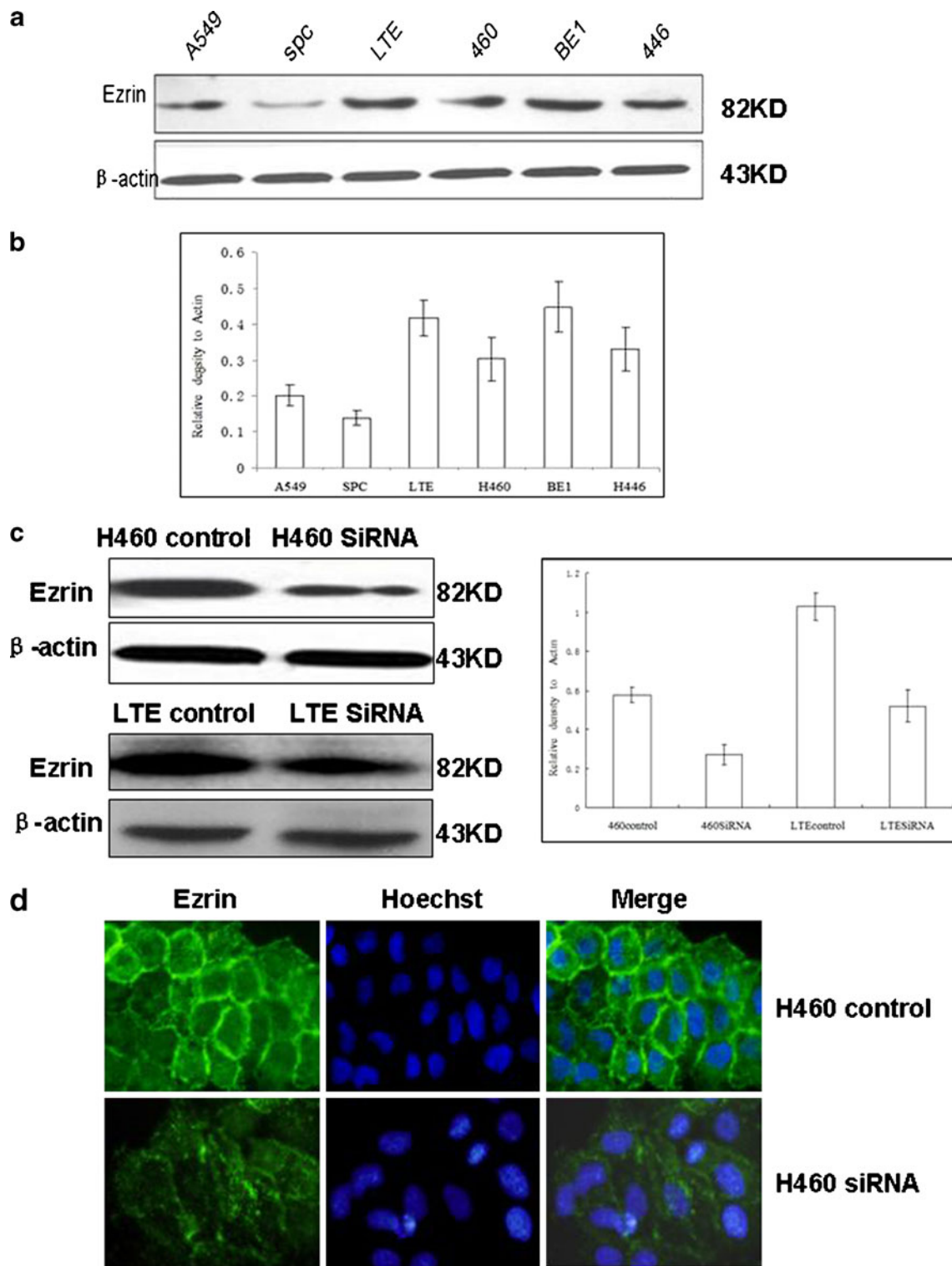


Fig. 1 Screening endogenous ezrin in six human lung cancer cell lines and transient knockdown of ezrin in H460 and LTE cell lines. **a**, **b** Ezrin protein expression in A549, SPC, LTE, H460, BE1, and H446 cell lines determined by Western blot analysis. **c** Western blot analysis of whole-cell lysates of H460 and LTE cell lines transfected with ezrin siRNA or scrambled siRNA. The ezrin protein in each cell lysate was analyzed by immunoblotting with antibodies against ezrin and β -actin as a reference control. Decreased ezrin expression was noted in both

H460 and LTE cell lines when the cells were transfected with ezrin siRNA. **d** Indirect immunofluorescence of ezrin protein in both H460 cells transfected with scrambled siRNA and ezrin siRNA. The cell nuclei were stained with Hoechst. Note predominant membranous staining of ezrin in the control group (*upper panel*) and a marked decrease in ezrin on the membrane after transfection with ezrin siRNA in the *lower panel*

Indirect immunofluorescence

Cells grown in 24-well plate were fixed with ice-cold 100 % methanol at -20°C for 15 min, followed by permeabilization with 0.2 % Triton X-100, and then were blocked with 1 % BSA in PBS for 1 h. β -catenin and E-cadherin were detected using mouse monoclonal antibodies against β -catenin (1:400, catalog number sc-59896, Santa Cruz, CA) or against E-cadherin (1:50, catalog number sc-8426, Santa Cruz, CA), respectively. Ezrin was detected using rabbit monoclonal antibodies (1:400, catalog number 1940-1, Epitomics biotech company, USA). Primary antibodies were applied overnight at 4°C followed by incubation

with a secondary antibody conjugated to rhodamine/FITC-labeled goat anti-mouse or anti-rabbit antibodies (1:100 each, ZhongShan Biotechnology, Beijing). The nuclei were counterstained with Hoechst 33342. The cells were examined with an Olympus IX51 fluorescent microscope (Olympus, Tokyo, Japan), and images were taken with a CoolPIX 5400 camera (Nikon, Japan).

RNA extraction and reverse transcriptase-polymerase chain reaction

Total RNA of the cultured cells was prepared using the TRIzol reagent (Invitrogen, Carlsbad, CA, USA). Reverse

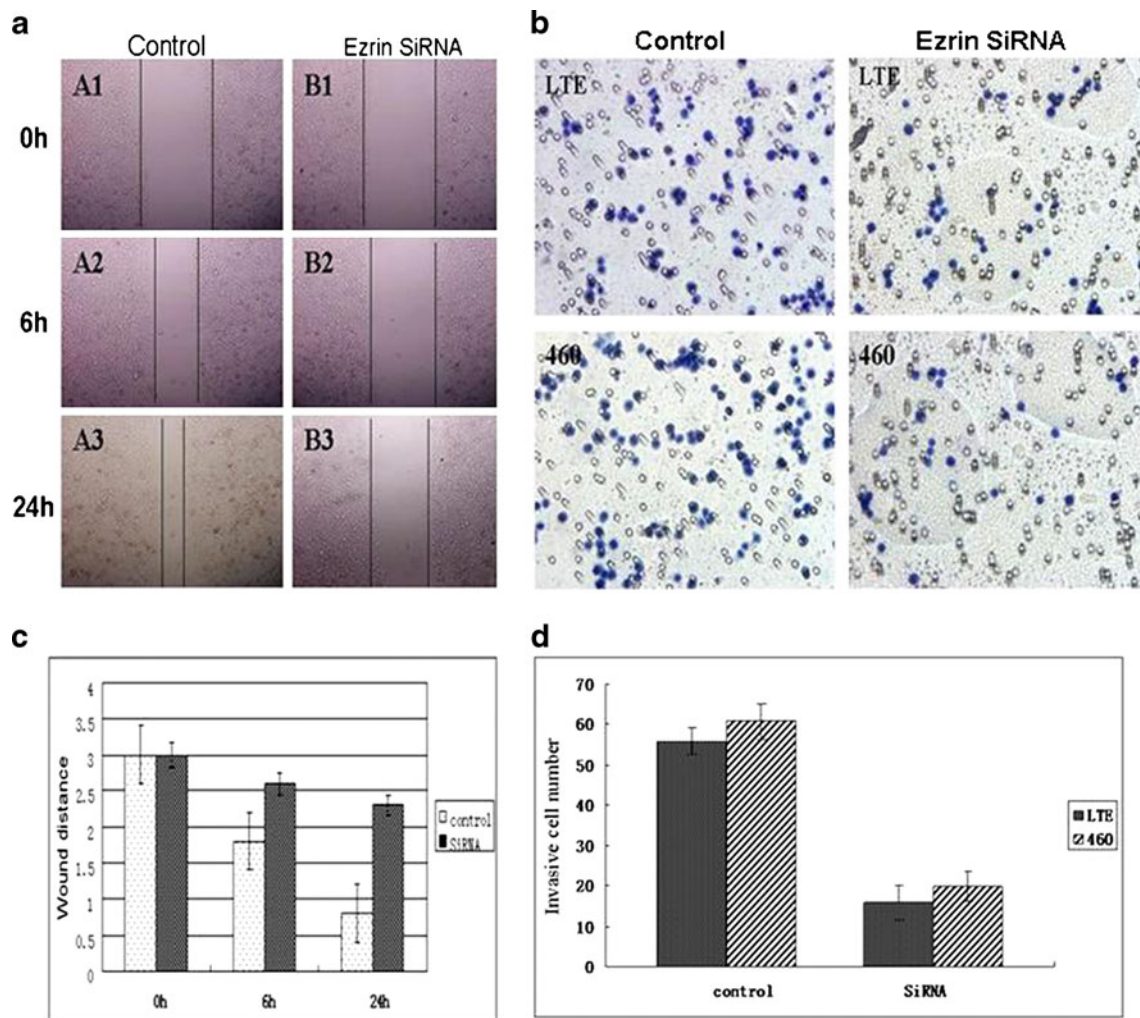
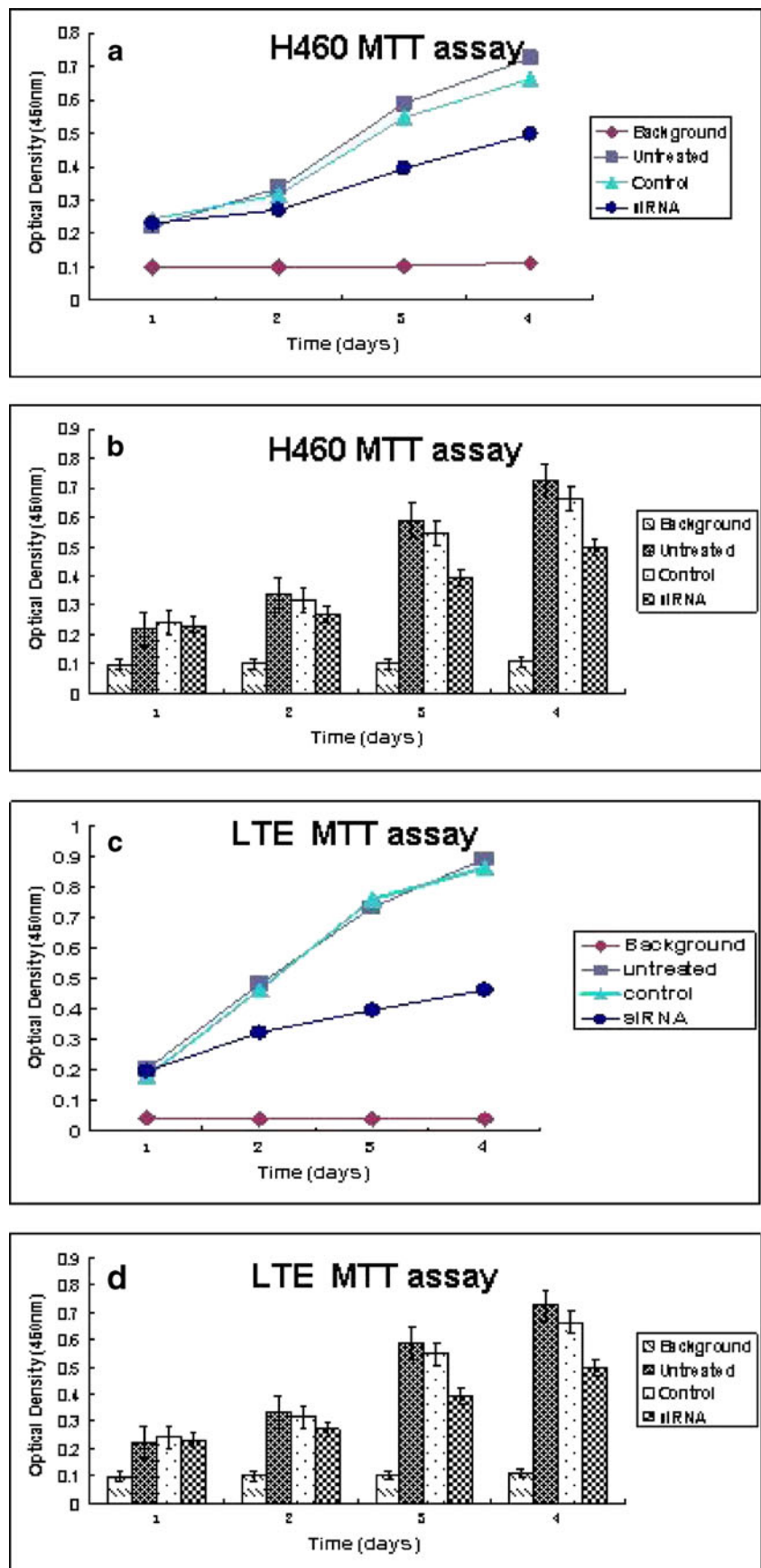


Fig. 2 Cell migration and invasive ability were detected by wound healing assay and transwell assay. **a** Confluent H460 cells transfected with either ezrin siRNA or control siRNA were scored using a micropipette tip, and spontaneous cell migration was monitored using a Nikon inverted microscope at 0, 6, and 24 h. **b** The H460 and LTE cells transfected with either ezrin siRNA or scrambled siRNA were seeded onto Matrigel-precoated filters of cell culture inserts and incubated for 16 h. The cells which reached the underside of the filters during

migration toward FBS were counted. **c, d** The distance of wound closure and the cells which reached the underside of the filters during invasion through Matrigel were counted. Relative cell motility and invasiveness are shown. Values from at least three independent experiments were pooled and expressed as means \pm SD. Delayed wound closure in the group treated with ezrin siRNA (**a, c**) and decreased invasiveness in both LTE and H460 cell lines after ezrin siRNA transfection (**b, d**) in comparison with control group were seen

Fig. 3 Cellular proliferation was measured with MTT assay. After the cells were transfected with ezrin siRNA or scrambled siRNA in LTE and H460 cells for 24, 48, 72, and 96 h, the absorbance was measured at 550 nm using a microplate reader. A blank reading with DMSO alone was taken as background. **a, c** Both LTE and H460 cells transfected with ezrin siRNA showed a reduced proliferation rate compared to cells transfected with scrambled siRNA (control group) and parent cells (untreated). **b, d** Statistical analysis of MTT results demonstrated that ezrin siRNA transfection decreased LTE and H460 cell proliferation ($P=0.0001$; $P=0.0028$, respectively) compared with the control group



transcriptase-polymerase chain reaction (RT-PCR) was performed using TaKaRa RNA PCR Kit (AMV) version 3.0 (TaKaRa Biotechnology Co., Ltd., Dalian, China) according to the manufacturers' protocols. The PCR products were electrophoresed in a 1.5 % agarose gel containing 0.1 $\mu\text{g}/\mu\text{l}$ EB. A grayscale intensity for each target band was normalized to the amplified product of β -actin RNA to provide a value for the transcriptional level of each gene.

Statistical analysis

Each experiment was performed three times. All of the data were expressed as mean \pm standard deviation (SD). Comparisons between groups were conducted using one-way analysis of variance followed by a least significant difference test. For multiple comparisons, either SPSS13 for Windows (SPSS Inc., Chicago, IL, USA) or Microsoft Excel was used. Chi-square test was employed to analyze ezrin's expression with clinicopathological factors. Differences were considered statistically significant when P value is <0.05 .

Results

Cell line selection and siRNA transfection

To analyze the function of ezrin in lung cancer cells, we first screened the expression of ezrin protein in six common lung cancer cell lines A549, SPC, LTE, H460, BE1, and H446. Among these, ezrin was highly expressed in high-metastatic cell lines LTE, BE1, H446, and H460, whereas it was weakly expressed in low-metastatic cell lines SPC and A549 cells (Fig. 1a, b), suggesting that ezrin expression may correlate directly with metastatic potential of human lung cancer cells. Thereafter, we chose LTE and H460 cell lines with higher expression to further investigate the effect of transient ezrin knockdown on tumor cell migration and invasion.

Knockdown of ezrin with siRNA duplexes in H460 and LTE (Fig. 1c) lung cancer cells reduced protein expression by 50 % compared to the controls transfected with scrambled siRNA duplex. No significant change of β -actin, which served as sample loading reference, was observed (Fig. 1c).

The ezrin protein in control cells was observed mainly on the cell membrane, while a small amount of ezrin was seen in the cytoplasm. Following ezrin siRNA transfection, the level of ezrin was markedly decreased on the cell membrane (Fig. 1d)

Ezrin knockdown significantly reduced cell migration, invasion and proliferation in LTE and H460 lung cancer cells in vitro

Increase in cancer cell migration and invasiveness is an important in vitro indication for aggressiveness and metastatic

potential of malignant tumors. We examined the role of ezrin in cell migration and invasion using the established LTE and H460 ezrin knockdown cells. Wound healing assays were performed to evaluate the cell migration ability after ezrin knockdown in H460 cells. A wound was created on a cell monolayer, and the wound closure was assessed at various time points up to 24 h. Transient knockdown of ezrin in H460 cells reduced the ability of wound repair by approximately threefold compared with the control group transfected with scrambled siRNA (Fig. 2a, c).

We further examined the effects of ezrin knockdown on cell invasion of LTE and H460 cells by using a matrigel-coated transwell assay. The cells invading into a matrigel-coated transwell membrane were counted 16 h after incubation. LTE and H460 cells transfected with ezrin siRNA showed reduced cell invasion by threefold compared to the cells transfected with scrambled siRNA, which exhibited a significantly higher level of invasion (Fig. 2b, d).

To investigate the effects of ezrin on growth of lung cancer cells, we measured the cell proliferation rate using the MTT assay at 24, 48, 72, and 96 h after LTE and H460

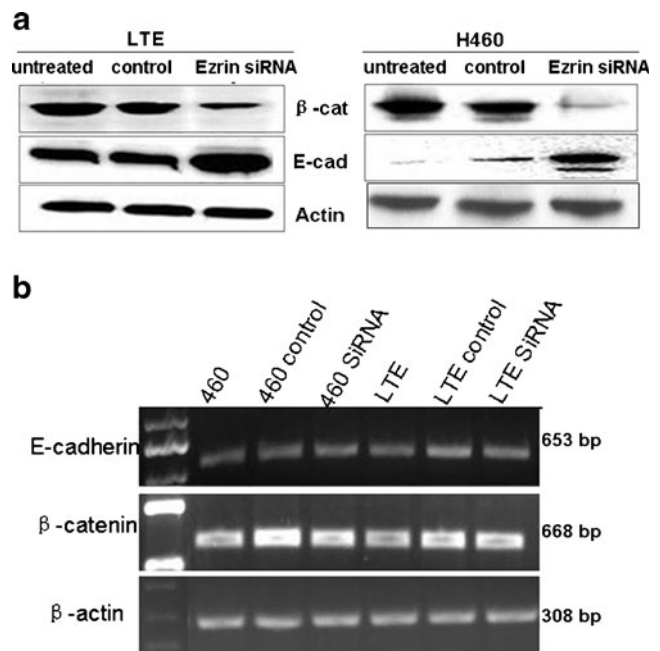


Fig. 4 Correlation of ezrin expression with cell adhesion molecules in H460 and LTE lung cancer cells. **a** Effect of ezrin on β -catenin and E-cadherin. Fifty micrograms of protein extract from cells transfected with ezrin siRNA or scrambled siRNA was loaded onto each lane of a 10 % SDS-PAGE, which was then subjected to immunoblotting with either anti-E-cadherin or anti- β -catenin antibodies. The level of β -actin was used as an internal control. Note ezrin siRNA significantly down-regulated β -catenin, while the expression of E-cadherin was up-regulated in both H460 and LTE cells. **b** Effect of ezrin on transcription of β -catenin and E-cadherin. Semi-qualitative RT-PCR was performed and showed no significant changes in mRNA of β -catenin and E-cadherin in both cell lines after transfection

cells were transfected with ezrin siRNA or scrambled siRNA. LTE and H460 cells transfected with ezrin siRNA showed a reduced proliferation rate compared to cells transfected with scrambled siRNA and parent cells (untreated) (Fig. 3a, c). Statistical analysis of MTT results demonstrated a significant reduction of cell proliferation in the cells with ezrin knockdown ($P=0.0001$, $P4=0.0028$, respectively) compared with corresponding controls (Fig. 3b, d).

Downregulation of ezrin reduced the expression of β -catenin but enhanced the expression of E-cadherin at posttranscriptional levels

It has been reported that ezrin plays a role in modulating the expression of β -catenin and E-cadherin in human breast and colorectal cancer cells. Here, we tested whether or not ezrin could affect β -catenin and E-cadherin levels in human lung cancer cells. By using Western blot analysis in LTE and H460 cells, we found that the expression of β -catenin was markedly reduced in ezrin knockdown cells, while the

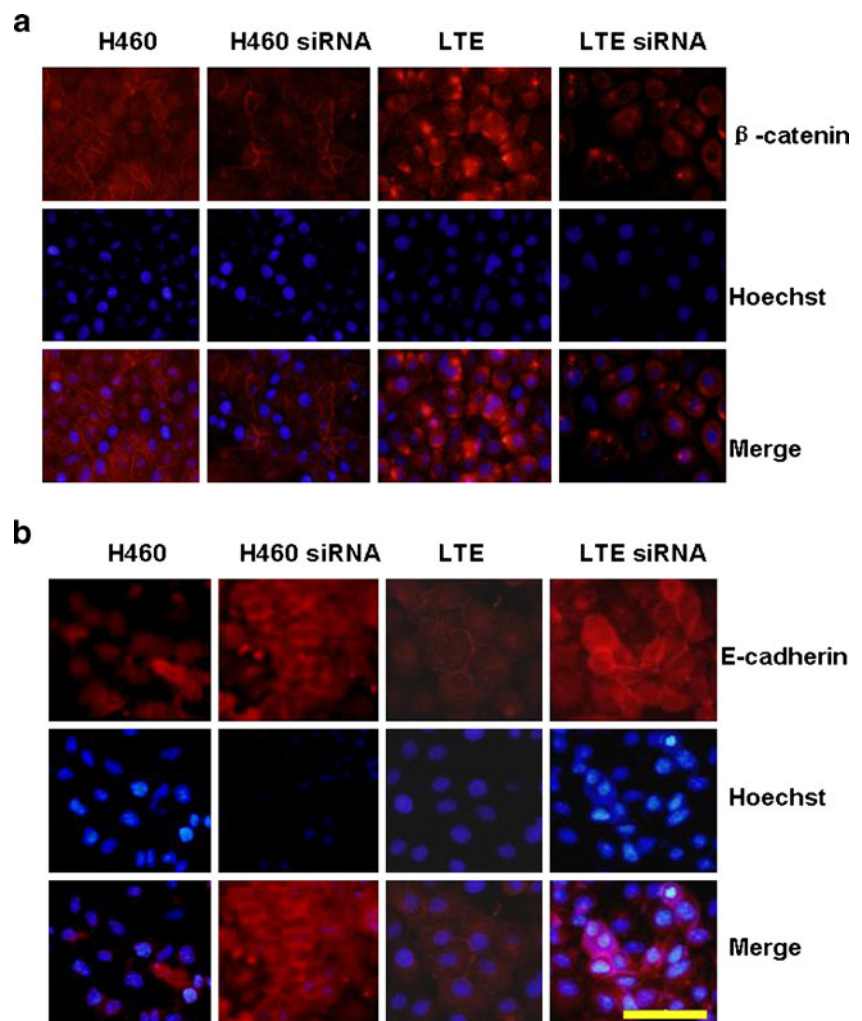
expression of E-cadherin was significantly increased compared to the corresponding control groups (Fig. 4a).

To investigate if the ezrin-mediated modulation of β -catenin and E-cadherin was at the transcriptional level, we performed RT-PCR to detect the mRNA levels of β -catenin and E-cadherin. As shown in Fig. 4b, ezrin knockdown did not alter the transcription of either β -catenin or E-cadherin in LTE and H460 cells.

Downregulation of ezrin enhanced membranous expression of E-cadherin and decreased cytoplasmic β -catenin

The effects of ezrin knockdown on β -catenin and E-cadherin were determined in both LTE and H460 cells by using indirect immunofluorescence to visualize changes of β -catenin and E-cadherin molecules following ezrin knockdown. Figure 5a shows that in the control cells, β -catenin is expressed both in the cytoplasm and on the cell membrane of H460 cells and mainly in the cytoplasm of LTE cells. Following transient ezrin knockdown, β -catenin in both cell

Fig. 5 Indirect immunofluorescence was conducted to visualize the localization of E-cadherin and β -catenin in the H460 and LTE cell lines after transfection with either ezrin siRNA or scrambled control siRNA. The cell nucleus was stained with Hoechst. Scale bar, 50 μ m. Note transient knockdown of ezrin enhanced cytomembranous expression of E-cadherin (**b**) and decreased cytoplasmic β -catenin (**a**)



lines was markedly decreased, particularly in the cytoplasm, with residual membranous staining. By immunofluorescence, E-cadherin was shown to be expressed at an extremely low level in LTE cells and to be localized mainly in the cytoplasm of H640 cells without significant membranous staining. Transient knockdown of ezrin demonstrated a marked increase in E-cadherin in both cell lines. Interestingly, intense membranous staining was noted in H460 cells following transfection with ezrin siRNA, suggesting relocalization of E-cadherin to the region of cell–cell adherens junctions, in addition to a quantitative increase of the protein (Fig. 5b).

Ezrin is expressed at higher levels in primary and metastatic lung cancer than normal lung tissue

To further investigate the role of ezrin in primary human lung cancer cells, we evaluated the expression of ezrin in 183 primary non-small cell lung cancers (NSCLC) and their paired autologous non-neoplastic (normal) tissues using immunohistochemical staining. In normal lung tissues, ezrin is

expressed mainly at the apical membrane of bronchiolar epithelium (Fig. 6a) and weakly expressed in alveolar epithelium (Fig. 6e). In contrast, in NSCLC tissues and metastatic foci, ezrin is expressed primarily in the cytoplasm (Fig. 6c). Furthermore, expression of ezrin was higher at the invasive front than in the central part of tumor mass (Fig. 6d) and was highest in lymphatic metastasis of lung cancer (Fig. 6b). These results suggest that ezrin localized to the cytoplasm may correlate with cell invasion and metastasis in NSCLC. Table 1 summarizes the immunohistochemical staining of ezrin in different types of lung NSCLC cancers. Of 93 patients with lymph node metastases, 88 (94.6 %) were positive for ezrin, in comparison to 73 (81.1 %) out of 90 patients without metastasis (N0 versus N1–3, $P=0.005$). Ezrin expression correlated directly to pTNM stage, with an increased tendency of ezrin expression in higher stages (83.9 % in stages I and II versus 94.4 % in stages III and IV, $P=0.032$). No significant correlation was found between ezrin expression and gender, age, histological type, or neoplastic differentiation.

Fig. 6 The expression patterns of ezrin in representative lung cancer, paired autologous non-neoplastic (normal) lung tissue, lymphatic metastatic foci, and the invasive front of tumor mass (streptavidin–peroxidase immunohistochemistry method, original magnification $\times 200$). In normal lung tissue (a), ezrin was mainly localized on the apical membrane of bronchial epithelium and weakly expressed in alveolar epithelium. In primary lung cancer (c) and lymphatic metastatic foci (b), ezrin was expressed primarily in the cytoplasm, with metastatic foci showing much stronger positivity than the primary lesion. More interestingly, in the invasive front of the tumor mass (d), ezrin was expressed at a much higher level than the central portion of the lesion (c). e Part of the tissue microarray specimen with columns 1, 3, and 5 representing the sampled tumor tissues (T) and columns 2, 4, and 6 being the paired autologous non-neoplastic (normal) tissues (N)

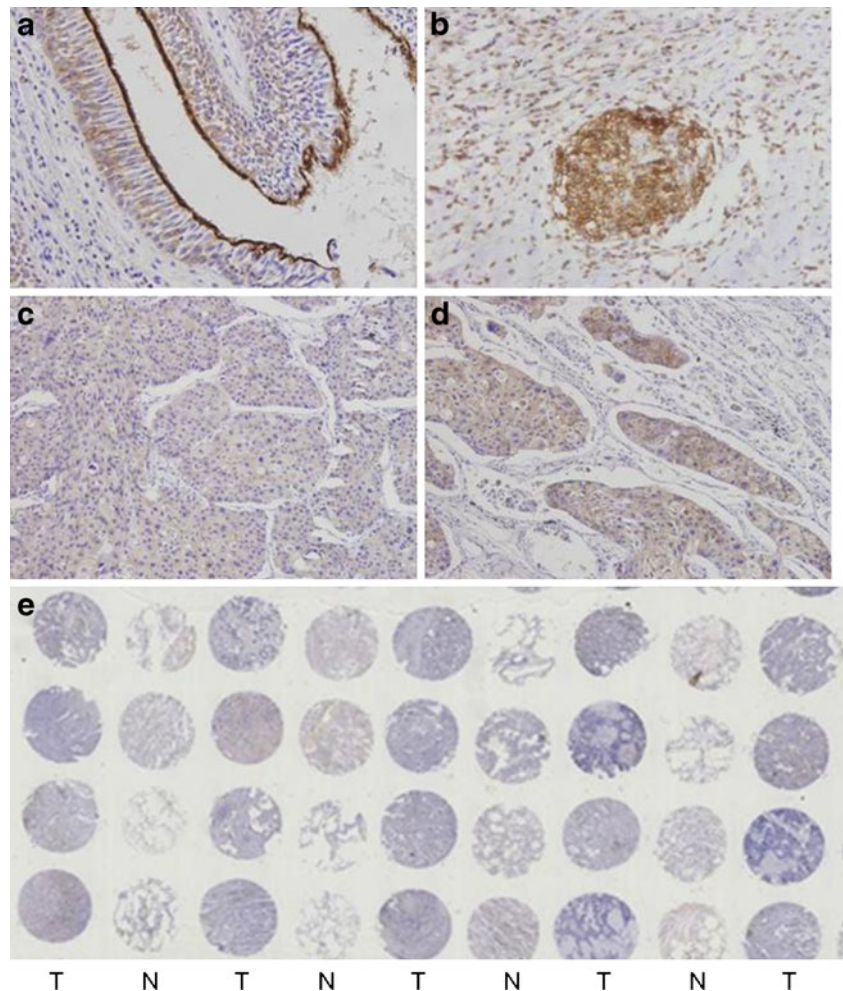


Table 1 The expression of ezrin in lung cancers

	No. of patients	Ezrin expression		
		Positive	Negative	<i>P</i> value
Gender				
Male	121	107	14	0.793
Female	62	54	8	
Age (year)				
≥65	86	73	13	0.226
<65	97	88	9	
Histological type				
Adenocarcinoma	102	93	9	0.492
Squamous cell carcinoma	36	33	3	
Adenosquamous carcinoma	10	8	2	
Bronchioloalveolar carcinoma	15	11	4	
Large cell carcinoma	10	8	2	
Small cell carcinoma	10	8	2	
Differentiation				
Poor	96	82	14	0.107
Well moderate	87	79	8	
Lymph node metastasis				
N0	90	73	17	0.005
N1–3	93	88	5	
pTNM status				
I + II	112	94	18	0.032
III + IV	71	67	4	

Discussion

Lung cancer is the most common cause of death in both men and women worldwide [20]. Local and distant metastases can occur even at early phases of the disease. The majority of patients have a poor prognosis, and the rate of complete cure is extremely low [21]. An understanding of the molecular mechanisms underlying tumor invasion and metastasis would have significant clinical implications on the diagnosis and treatment of lung cancer. Ezrin acts as a linker between the other cell membrane proteins and the cytoskeleton element actin and has been reported to play a unique role in cell signaling transduction, development, and differentiation. The ezrin molecule has been particularly implicated to play a role in tumor cell invasion and metastasis [4]. Recent histological studies have demonstrated a correlation of ezrin expression with a malignant phenotype in a number of cancers, including carcinomas of endometrium, breast, colon, and ovary, as well as uveal and cutaneous melanoma, brain tumors, and most recently, soft tissue sarcomas [9].

The role of ezrin expression in lung cancer cells has seldom been previously studied [22], and for the first time, we conducted *in vitro* migration and invasion assays in two lung cancer cell lines LTE and H460 by manipulating levels of ezrin protein. Our results showed that ezrin knockdown

by siRNA significantly reduced the ability for migration and invasion in LTE and H460 lung cancer cells. It has been previously demonstrated that ezrin, a cytoskeletal protein, might be involved in regulating the assembly of cytoskeletal elements on the interior portion of cell membranes and in the nucleus, hence, facilitating cell migration and invasion [23]. The data in the current study were in agreement with and complementary to the previous reports demonstrating that changes in the cytoskeleton might be a key factor in regulating neoplastic progression and tumor growth [24]. Two other previous studies have shown the crucial role of ezrin in regulating metastasis in two highly metastatic cancers, osteosarcoma and rhabdomyosarcoma [8, 25]. More interestingly, recent studies have suggested that ezrin is dynamically regulated during different stages of osteosarcoma metastasis [26]. Ezrin is upregulated during early development of metastasis but is downregulated during the intervening establishment and survival of metastatic foci, suggesting its role in junctional remodeling and/or stability [27]. Our study showed that disrupted expression of ezrin *in vitro* correlated with a decrease in anchorage-independent growth of lung cancer cells (Fig. 2a), which is in agreement with the previous finding in glioma cells [28].

Ezrin participates in several crucial signal transduction pathways, including the MAPK, AKT, Rho kinase, and

CD44 pathways, promoting cytoskeletal reorganization and subsequent phenotypic alterations in cells [4]. Previous studies have shown that ezrin plays a pivotal role in expression and localization of the adhesion molecules E-cadherin and β -catenin. E-cadherin is a key component in cell–cell adhesion and maintenance of cell colony integrity in epithelial cells [29]. It has been well documented that loss of or inhibition of the function of E-cadherin or its associated proteins, the catenins, results in reduced intercellular adhesion and a gain in invasive potential [30]. In the present study, we demonstrated that downregulation of ezrin reduced the protein expression of β -catenin but enhanced the expression of E-cadherin (Fig. 4a) with no effect at their transcriptional levels in two lung cancer cell lines H460 and LTE (Fig. 4b). This suggests posttranscriptional regulation of these two cell adhesion molecules by ezrin. Moreover, transient knockdown of ezrin in the two lung cancer cells with relatively high endogenous ezrin showed an increase in E-cadherin expression, particularly on the cell membrane, and decreased β -catenin in the cytoplasm. Interestingly, untreated H460 cells had their E-cadherin localized mainly in the cytoplasm, while disrupted expression of ezrin in this cell line not only enhanced the level of E-cadherin but also redistributed it to the cell membrane (Fig. 5b). Although enhanced E-cadherin activity by stabilizing or redistributing it on the cell membrane may be a crucial step in this process, the underlying mechanisms by which ezrin regulates the expression and/or localization of the E-cadherin/ β -catenin complex and a malignant phenotype remain to be further investigated.

There is evidence of pleiotropic function of ezrin in malignant tumors [31] and in fact, while the ezrin involvement in tumor cell migrating ability is well understood, some other ezrin-mediated tumor cell activity is still to be elucidated, such as the role of ezrin in tumor cell cannibalism [32] and in multidrug resistance [33]. Moreover, ezrin is normally involved in death receptor-mediated apoptosis [34] and it appears conceivable that aberrant ezrin expression may be also involved in the reduced sensitivity of tumor cells to apoptotic stimuli. Thus, while it is extremely clear that ezrin is directly involved with the capacity of tumor cells to migrate through tissues and vessels [35], more wide involvement of ezrin in tumor malignancy [36] should be more extensively concerned.

In the present study, expression levels of ezrin protein were found to be significantly higher in primary cancer tissues than paired autologous normal lung tissue, supporting a possible role of ezrin in lung cancer development. Interestingly, ezrin protein was seen mainly in the apical membrane of normal bronchial epithelium but primarily in the cytoplasm of both primary lung cancer cells and metastatic cancer cells, suggesting the importance of the subcellular localization of ezrin protein in human lung cancers, particularly in metastatic cancer. In addition, the expression

of ezrin was much higher in the invasive front of primary lesions of lung cancer than the central portion of the tumor mass (Fig. 6c, d), and the highest expression was seen in the lymphatic metastasis of lung cancer (Fig. 6b). These findings are in agreement with those observed previously in different malignancies [25] and support the notion that ezrin protein is dynamically regulated during different stages of malignancy. In addition, the level or distribution of ezrin in cells may determine not only the phenotype of the cells but also the biological behavior of the neoplastic cells. Statistical analyses of data from tissue microarray assays revealed a strong correlation between the expression of ezrin and clinical stages (stage I/II versus stage III/IV, $P=0.032$) or status of lymph node metastasis (N0 versus N1–3, $P=0.005$) in lung cancer patients (Table 1). These findings suggest that immunohistochemical evaluation of ezrin may be used as one prognostic marker in predicting clinical outcome of lung cancer patients.

Financial support This study received financial support from the National Natural Science Foundation of China (grant no. 30700806 to Q-C Li).

Conflicts of interest None

References

- Berghmans T, Dusart M, Paesmans M, Hossein-Foucher C, Buvat I, Castaigne C. Primary tumor standardized uptake value (SUV-max) measured on fluorodeoxyglucose positron emission tomography (FDG-PET) is of prognostic value for survival in non-small cell lung cancer (NSCLC): a systematic review and meta-analysis (MA) by the European Lung Cancer Working Party for the IASLC Lung Cancer Staging Project. *J Thorac Oncol.* 2008;3:6–12.
- Shibue T, Weinberg RA. Metastatic colonization: settlement, adaptation and propagation of tumor cells in a foreign tissue environment. *Semin Cancer Biol.* 2011;21:99–106.
- Lallemant D, Arpin M. Moesin/ezrin: a specific role in cell metastasis? *Pigm Cell Melanoma R.* 2010;23:6–7.
- Neisch AL, Fehon RG. Ezrin, Radixin and Moesin: key regulators of membrane–cortex interactions and signaling. *Curr Opin Cell Biol.* 2011;23:377–82.
- Huang HY, Li CF, Fang FM, Tsai JW, Li SH, Lee YT, et al. Prognostic implication of ezrin overexpression in myxofibrosarcomas. *Ann Surg Oncol.* 2010;17:3212–9.
- Xie JJ, Xu LY, Xie YM, Zhang HH, Cai WJ, Zhou F, et al. Roles of ezrin in the growth and invasiveness of esophageal squamous carcinoma cells. *Int J Cancer.* 2009;124:2549–58.
- Ohtani K, Sakamoto H, Rutherford T, Chen Z, Kikuchi A, Yamamoto T, et al. Ezrin, a membrane–cytoskeletal linking protein, is highly expressed in atypical endometrial hyperplasia and uterine endometrioid adenocarcinoma. *Cancer Lett.* 2002;179:79–86.
- Khanna C, Wan X, Bose S, Cassaday R, Olomu O, Mendoza A, et al. The membrane–cytoskeleton linker ezrin is necessary for osteosarcoma metastasis. *Nat Med.* 2004;10:182–6.
- Ana C, Bendahl PO, Åkerman M, Domanski HA, Rydholm A, Engellau J, et al. Ezrin expression predicts local recurrence and

- development of metastases in soft tissue sarcomas. *J Clin Pathol.* 2011;64:689–94.
10. Hunter KW. Ezrin, a key component in tumor metastasis. *Trends Mol Med.* 2004;10:201–4.
 11. Kocher HM, Sandle J, Mirza TA, Li NF, Hart IR. Ezrin interacts with cortactin to form podosomal rosettes in pancreatic cancer cells. *Gut.* 2009;58:271–84.
 12. Osawa H, Smith CA, Ra YS, Kongkham P, Rutka JT. The role of the membrane cytoskeleton cross-linker ezrin in medulloblastoma cells. *Neuro-Oncology.* 2009;11:381–93.
 13. Ohtani K, Sakamoto H, Rutherford T, Chen Z, Satoh K, Naftolin F. Ezrin, a membrane–cytoskeletal linking protein, is involved in the process of invasion of endometrial cancer cells. *Cancer Lett.* 1999;147:31–8.
 14. Martin M, Andreoli C, Sahuquet A, Montcourrier P, Algrain M, Mangeat P. Ezrin Nh2-terminal domain inhibits the cell extension activity of the cooh-terminal domain. *J Cell Biol.* 1995;128:1081–93.
 15. Li Q, Wu M, Wang H, Xu G, Zhu T, Zhang Y, et al. Ezrin silencing by small hairpin RNA reverses metastatic behaviors of human breast cancer cells. *Cancer Lett.* 2008;261:55–63.
 16. Helander TS, Carpen O, Turunen O, Kovanen PE, Vaheri A, Timonen T. ICAM-2 redistributed by ezrin as a target for killer cells. *Nature.* 1996;382:265–8.
 17. Pujuguet P, Maestro LD, Gautreau A, Louvard D, Arpin M. Ezrin regulates E-cadherin-dependent adherens junction assembly through Rac1 activation. *Mol Biol Cell.* 2003;14:2181–91.
 18. Allenspach EJ, Cullinan P, Tong J, Tang Q, Tesciuba AG, Cannon JL, et al. ERM-dependent movement of CD43 defines a novel protein complex distal to the immunological synapse. *Immunity.* 2001;15:739–50.
 19. Mackay DJG, Esch F, Furthmayr H, Hall A. Rho-and Rac-dependent assembly of focal adhesion complexes and actin filaments in permeabilized fibroblasts: an essential role for ezrin/radixin/moesin proteins. *Cell Biol.* 1997;138:927–38.
 20. Stratton MR. Exploring the genomes of cancer cells: progress and promise. *Science.* 2011;331:1553–8.
 21. William NJ, Glisson BS. Novel strategies for the treatment of small-cell lung carcinoma. *Nat Rev Clin Oncol.* 2011;8:611–9.
 22. Zhang XQ, Chen GP, Wu T, Yan JP, Zhou JY. Expression and clinical significance of ezrin in non-small-cell lung cancer. *Clin Lung Cancer.* 2011 Dec 1. doi:10.1016/j.clcc.2011.04.002.
 23. Bretscher A, Reczek D, Berryman M. Ezrin: a protein requiring conformational activation to link microfilaments to the plasma membrane in the assembly of cell surface structures. *J Cell Sci.* 1997;110:3011–8.
 24. Chen L, Hughes RA, Baines AJ, Conboy J, Mohandas N, An X. Protein 4.1R regulates cell adhesion, spreading, migration and motility of mouse keratinocytes by modulating surface expression of beta 1 integrin. *J Cell Sci.* 2011;124:2478–87.
 25. Yu Y, Khan J, Khanna C, Helman L, Meltzer PS, Merlino G. Expression profiling identifies the cytoskeletal organizer ezrin and the developmental homeoprotein Six-1 as key metastatic regulators. *Nat Med.* 2004;10:175–81.
 26. Ren L, Hong SH, Cassavaugh J, Osborne T, Chou AJ, Kim SY, et al. The actin–cytoskeleton linker protein ezrin is regulated during osteosarcoma metastasis by PKC. *Oncogene.* 2009;28:792–802.
 27. Estecha A, Sanchez-Martin L, Puig-Kroeger A, Bartolome RA, Teixido J, Samaniego RL, et al. Moesin orchestrates cortical polarity of melanoma tumour cells to initiate 3D invasion. *J Cell Sci.* 2009;122:3492–501.
 28. Tynninen O, Carpen O, Jaaskelainen J, Paavonen T, Paetau A. Ezrin expression in tissue microarray of primary and recurrent gliomas. *Neuropathol Appl Neuro.* 2004;30:472–7.
 29. Takeichi M, Watabe M, Shibamoto S, Ito F, Oda H, Uemura T, et al. Dynamic control of cell–cell adhesion for multicellular organization. *C R Acad Sci III.* 1993;316:818–21.
 30. Nagafuchi A, Ishihara S, Tsukita S. The roles of catenins in the cadherin-mediated cell adhesion: functional analysis of E-cadherin–alpha catenin fusion molecules. *J Biol Chem.* 1994;127:235–45.
 31. Federici C, Brambilla D, Lozupone F, Matarrese P, de Milito A, Lugini L, et al. Pleiotropic function of ezrin in human metastatic melanomas. *Int J Cancer.* 2009;124:2804–12.
 32. Lugini L, Matarrese P, Tinari A, Lozupone F, Federici C, Iessi E, et al. Cannibalism of live lymphocytes by human metastatic but not primary melanoma cells. *Cancer Res.* 2006;66:3629–38.
 33. Brambilla D, Zamboni S, Federici C, Lugini L, Lozupone F, Milito AD, Cecchetti S, Cianfriglia M, Fais S. P-glycoprotein binds to ezrin at amino acid residues 149–242 in the FERM domain and plays a key role in the multidrug resistance of human osteosarcoma. *Int J Cancer.* 2011, doi: 10.1002/ijc.26285.
 34. Parlato S, Giammarioli AM, Logozzi M, Lozupone F, Matarrese P, Luciani F, et al. CD95 (APO-1/Fas) linkage to the actin cytoskeleton through ezrin in human T lymphocytes: a novel regulatory mechanism of the CD95 apoptotic pathway. *EMBO J.* 2000;19:5123–34.
 35. Fais S. Moulding the shape of a metastatic cell. *Leuk Res.* 2010;34:843–7.
 36. Brambilla D, Fais S. The Janus-faced role of ezrin in “linking” cells to either normal or metastatic phenotype. *Int J Cancer.* 2009;125:2239–45.